Article

Functionalization of Thioctic Acid-Capped Gold Nanoparticles for Specific Immobilization of Histidine-Tagged Proteins

Jos M. Abad, Stijn F. L. Mertens, Marcos Pita, Victor M. Fernndez, and David J. Schiffrin

J. Am. Chem. Soc., **2005**, 127 (15), 5689-5694• DOI: 10.1021/ja042717i • Publication Date (Web): 19 March 2005

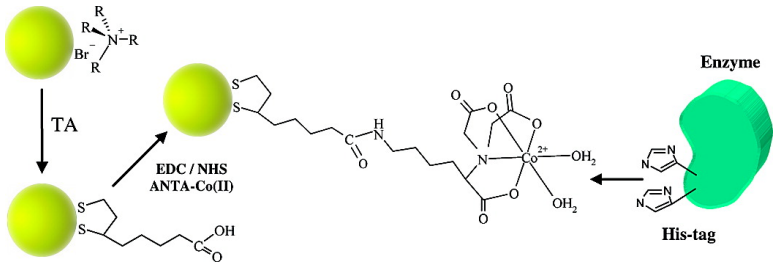

More About This Article

Additional resources and features associated with this article are available within the HTML version:

- Supporting Information
- Links to the 12 articles that cite this article, as of the time of this article download
- Access to high resolution figures
- Links to articles and content related to this article
- Copyright permission to reproduce figures and/or text from this article

View the Full Text HTML

J|A|C|S
ARTICLES
Published on Web 03/19/2005

Functionalization of Thioctic Acid-Capped Gold Nanoparticles for Specific Immobilization of Histidine-Tagged Proteins

José M. Abad,*[,†,§] Stijn F. L. Mertens,[‡] Marcos Pita,[†] Victor M. Fernández,[†] and David J. Schiffrin[‡]

Contribution from the Instituto de Catálisis y Petroleoquímica, CSIC, C/Marie Curie 2, 28049 Madrid, Spain, and Centre for Nanoscale Science, Chemistry Department, University of Liverpool, Liverpool L69 7ZD, United Kingdom

Received December 3, 2004; E-mail: jmabad@icp.csic.es

Abstract: This paper presents an efficient strategy for the specific immobilization of fully functional proteins onto the surface of nanoparticles. Thioctic acid-derivatized gold clusters are used as a scaffold for further stepwise modification, leading to a cobalt(II)-terminated ligand shell. A histidine tag introduced by genetic engineering into a protein is coordinated to this transition metal ion. The specific immobilization has been demonstrated for the cases of a genetically engineered horseradish peroxidase and ferredoxin-NADP$^+$ reductase, confirming the attachment of the fully functional proteins to the Co(II)-terminated nanointerface. The absence of nonspecific protein adsorption and the specificity of the binding site have been verified using several analogues of the enzymes without the histidine tag.

1. Introduction

There is a growing interest in the use of nanoparticles modified with biomolecules for the rational design of nanostructured functional materials[1] and their use in electronic, optical, and biosensor applications. Metallic and semiconductor nanoparticles can now be synthesized from a wide range of materials, showing fascinating properties resulting from their small dimensions.[2] There are two key requirements for obtaining stable nanoparticle−biomolecule conjugates. First, the synthesis of water-dispersible metallic nanoparticles of controlled size and shape in concentrated aqueous solutions is desirable to achieve extensive biomolecule−nanoparticle conjugation. Synthetic methods in an organic phase[3] are often preferable, as they yield better particle monodispersity and higher particle concentrations than water-based preparations.[4] In addition, these avoid agglomeration problems associated with ionic interactions. Once synthesized, efficient transfer of the colloid to an aqueous medium is required for further assembly of the bioconjugates. Thiol chemistry has been repeatedly used for this purpose.[5]

The second key challenge is to control the organization of biomolecules (such as enzymes, antigens, antibodies, DNA, receptors) on nanoparticles while retaining their biological activity. For DNA, successful attachment for detection purposes and as elemental building blocks in materials syntheses schemes has been achieved.[6] However, in the case of proteins (antibodies, enzymes, receptors), the methods commonly employed (nonspecific adsorption,[4c,7a,b] covalent attachment[7c,d]) are difficult to control and usually yield randomly bound proteins. An ideal immobilization strategy should clearly be based on specific interactions between the biological target molecule and tailored modifications of the nanoparticle surface, producing specific protein attachment in a favorable orientation for catalysis

† CSIC.
‡ University of Liverpool.
§ Present address: Centre for Nanoscale Science, Chemistry Department, University of Liverpool, Liverpool L69 7ZD, United Kingdom.

(1) (a) Katz, E.; Willner, I. *Angew. Chem., Int. Ed.* **2004**, *43*, 6042−6108. (b) Niemeyer, C. M.; Burger, W.; Peplies, J. *Angew. Chem., Int. Ed.* **2000**, *37*, 2265−2268. (c) Niemeyer, C. M., *Angew. Chem., Int. Ed.* **2001**, *40*, 4128−4158. (d) Mann, S.; Shenton, W.; Li, M.; Connolly, S.; Fitzmaurice, D. *Adv. Mater.* **2000**, *12*, 147−150. (e) Caruso, F. *Adv. Mater.* **2001**, *13*, 11−22. (f) Penn, S. G.; He, L.; Natan, M. J. *Curr. Opin. Chem. Biol.* **2003**, *7*, 609−615. (g) Taton, T. A. *Trends Biotechnol.* **2002**, *20*, 277−279. (h) Xiao, Y.; Patolsky, F.; Katz, E.; Hainfeld, J. F.; Willner, I. *Science* **2003**, *299*, 1877−1881.

(2) (a) Daniel, M.-C.; Astruc, D. *Chem. Rev.* **2004**, *104*, 293−346. (b) Murray, C. B.; Kagan, C. R.; Bawendi, M. G. *Annu. Rev. Mater. Sci.* **2000**, *30*, 545−610. (c) Liz-Marzán, L. M. *Mater. Today* **2004**, *Feb*, 26−31. (d) Alivisatos, A. P. *Science* **1996**, *271*, 933−937. (e) Schmid, G.; Chi, L. F. *Adv. Mater.* **1998**, *10*, 515−527. (f) Kamat, P. V. *J. Phys. Chem. B* **2002**, *106*, 7729−7744.

(3) (a) Schmid, G.; Pfeil, R.; Boese, R.; Bandermann, F.; Meyer, S.; Calis, S. G.; van der Velden, J. W. A. *Chem. Ber.* **1981**, *114*, 5634. (b) Brust, M.; Kiely, C. J. *Colloids Surf., A* **2002**, *202*, 175−186. (c) Brust, M.; Walker, M.; Bethell, D.; Schiffrin, D. J.; Whyman, R. *J. Chem Soc., Chem. Commun.* **1994**, 801−802. (d) Brust, M.; Walker, M.; Bethell, D.; Schiffrin, D. J.; Kiely, C. J. *J. Chem Soc., Chem. Commun.* **1995**, 1655.

(4) (a) Turkevitch, J.; Stevenson, P. C.; Hiller, J. *Discuss. Faraday Soc.* **1951**, *11*, 55−75. (b) Frens, G. *Nature: Phys. Sci.* **1973**, *241*, 20−22. (c) Hayat, M. A. *Colloidal Gold: Principles, Methods and Applications*; Academic Press: New York, 1989 (three volumes).

(5) (a) Schmid, G. *Polyhedron* **1988**, *7*, 2321. (b) Schmid, G.; Peschel, S.; Sawitowski, T. *Z. Anorg. Allg. Chem.* **1997**, *623*, 719. (c) Gittins, D. I.; Caruso, F. *ChemPhysChem* **2002**, *1*, 110−113. (d) Gittins, D. I.; Caruso, F. *Angew. Chem., Int. Ed.* **2001**, *40*, 3001. (e) De la Fuente, J. M.; Barrientos, A. G.; Rojas, T. C.; Rojo, R.; Cañada, J.; Fernández, A.; Penadés, S. *Angew. Chem., Int. Ed.* **2001**, *40*, 2257.

(6) (a) Storhoff, J. J.; Mirkin, C. A. *Chem. Rev.* **1999**, *99*, 1849−1862. (b) Mirkin, C. A. *Inorg. Chem.* **2000**, *39*, 2258−2272. (c) Kanaras, A. G.; Wang, Z.; Cosstick, A. D. B. R.; Brust, M. *Angew. Chem., Int. Ed.* **2003**, *42*, 191−194.

(7) (a) Anand Gole, A.; Dash, C.; Soman, C.; Sainkar, S. R.; Rao, M.; Sastry, M. *Bioconjugate Chem.* **2001**, *12*, 684−690. (b) Mattoussi, H.; Mauro, J. M.; Goldman, E. R.; Anderson, G. P.; Sundar, V. C.; Mikulec, F. V.; Bawendi, M. G. *J. Am. Chem. Soc.* **2000**, *122*, 12142−12150. (c) Patel, N.; Davies, M. C.; Hartshorne, M.; Heaton, R. J.; Roberts, C. J.; Tendler, S. J. B.; Williams, P. M. *Langmuir* **1997**, *13*, 6485−6490. (d) Keating, C. D.; Kovaleski, K. M.; Natan, M. J. *J. Phys. Chem. B* **1998**, *102*, 9404−9413.

Scheme 1. Reaction Strategy Showing the Successive Steps for the Construction of NTA-Terminated Nanoparticles for Specific Immobilization of Histidine-Tagged Proteins

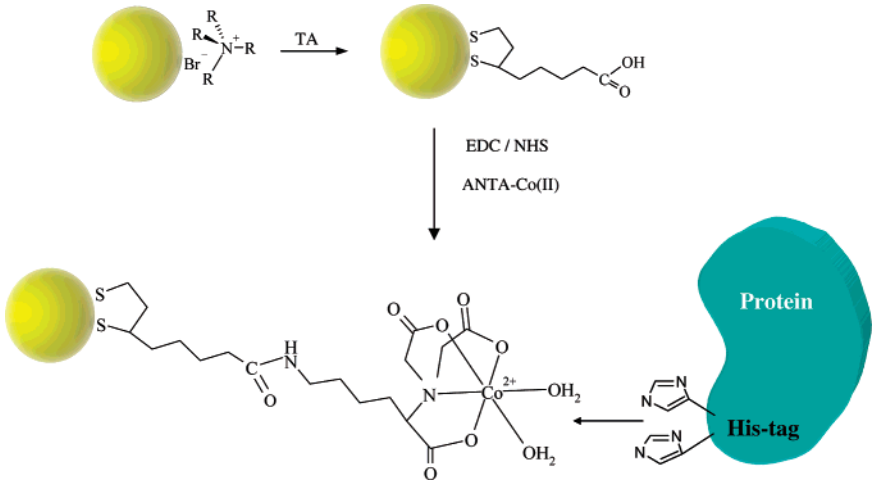

(enzymes) or binding (antibodies, receptors), while avoiding nonspecific protein adsorption.[8]

Self-assembled monolayers (SAMs)[9a] of alkanethiols allow the drastic reduction of nonspecific protein adsorption on macroscopic gold surfaces.[9b,c] Furthermore, the introduction of ligands in the SAM that are complementary to specific binding sites in either native proteins[9d] or genetically engineered analogues[9e−g] is an attractive avenue for their alignment and orientation.

The present work takes this idea one step further by using self-assembly on nanoparticles for the specific immobilization of functional proteins. The strategy followed is outlined in Scheme 1. Gold clusters are synthesized in an organic phase and transferred to water using lipoic acid, resulting in stable water-dispersible nanoparticles. Using the thiol-capped clusters as a building platform, a chemical modification of the ligand shell results in a nitrilotriacetic acid termination, which is suitable for complexation with transition metal ions. Proteins carrying histidine tags can then be readily attached to this transition metal complex.

The concept of histidine-tagged protein attachment to a transition metal terminated nitrilotriacetate group has been recently explored by Xu et al. using magnetic nanoparticles as substrate.[10] Their approach, however, involves rather lengthy and elaborate syntheses of the protein-immobilizing ligands. Our strategy offers, apart from time-efficiency, the distinct advantage of achieving the nanoparticle-NTA coupling in a single step.

In the present study, the specific immobilization properties of the material prepared were tested using two well-known enzymes: horseradish peroxidase (HRP) and ferredoxin-$NADP^+$ reductase (FNR). The oxidoreductase HRP contains a heme group and is known to participate in a two-step enzymatic reaction with H_2O_2 and a large number of electron donors.[11] Furthermore, its crystal structure has been determined, and this has enabled the preparation of nonglycosylated wild recombinant N_{His}-HRP_{rec} containing a six-histidine tag at the N-terminus of the enzyme by genetic engineering.[12] Finally, the availability of the unglycosilated recombinant (HRP_{rec}) and glycosylated commercial proteins (HRP_{com}) without His tags allows control experiments to verify the specificity of the immobilization strategy developed. Ferredoxin-$NADP^+$ reductase (FNR), on the other hand, catalyzes the reduction of $NADP^+$ to NADPH in two successive one-electron steps during the operation of photosystem I. This protein was genetically engineered to provide a couple of accessible histidine residues. Previous work with FNR mutants has shown that enzyme molecule orientation on an NTA-gold surface is dictated by the position of the histidine tag.[9e]

2. Experimental Section

All chemicals were obtained from commercial sources and used as received. MilliQ water (Millipore) was used throughout.

2.1. Synthesis of Thiol Derivatized Gold Nanoparticles. Au clusters were synthesized in toluene[3d] by the two-phase reduction of aqueous $HAuCl_4$ (3 cm^3, 30 mM, Aldrich), transferred to the organic phase using tetra-*n*-octylammonium bromide (TOABr) in toluene (8 cm^3, 50 mM, Fluka), and reduced with aqueous sodium borohydride (2.5 cm^3, 0.4 M, Aldrich). Cluster derivatization was carried out by overnight incubation in a 0.1 M solution of 6,8-dithioctic acid (TA, Sigma) or 11-mercaptoundecanoic acid (MUA, Sigma) in toluene. The

(8) (a) Zheng, M.; Zhigang, L.; Huang, X. *Langmuir* **2004**, *20*, 4226−4235. (b) Boal, A. K.; Rotello, V. M. *J. Am. Chem. Soc.* **2000**, *122*, 734−735. (c) Schroedter, A.; Weller, H. *Angew. Chem., Int. Ed.* **2002**, *41*, 3218−3221. (d) Lévy, R.; Thanh, N. T. K.; Doty, R. C.; Hussain, I.; Nichols, R. J.; Schiffrin, D. J.; Brust, M.; Fernig, D. G. *J. Am. Chem. Soc.* **2004**, *126*, 10076−10084.

(9) (a) Ulman, A. *Chem. Rev.* **1996**, *96*, 1533−1554. (b) Prime, K. L.; Whitesides, G. M. *J. Am. Chem. Soc.* **1993**, *115*, 10714−10721. (c) Lahiri, J.; Isaacs, L.; Tien, J.; Whitesides, G. M. *Anal. Chem.* **1999**, *71*, 777−790. (d) Abad, J. M.; Velez, M.; Santamaria, C.; Guisan, J. M.; Matheus, P. R.; Vazquez, L.; Gazaryan, I.; Gorton, L.; Gibson, T.; Fernandez, V. M. *J. Am. Chem. Soc.* **2002**, *124*, 12845−12853. (e) Madoz-Gurpide, J.; Abad, J. M.; Fernandez-Recio, J.; Velez, M.; Vazquez, L.; Gomez-Moreno, C.; Fernandez, V. M. *J. Am. Chem. Soc.* **2000**, *122*, 9808−9817. (f) Madoz, J.; Kuznetzov, B. A.; Medrano, F. J.; Garcia, J. L.; Fernandez, V. M. *J. Am. Chem. Soc.* **1997**, *119*, 1043−1051. (g) Johnson, D. L.; Martin, L. L. *J. Am. Chem. Soc.* **2005**, *127*, 2018−2019.

(10) (a) Xu, C.; Xu, K.; Gu, H.; Zhong, X.; Guo, Z.; Zheng, R.; Zhang, X.; Xu, B. *J. Am. Chem. Soc.* **2004**, *126*, 3392−3393. (b) Xu, C.; Xu, K.; Gu, H.; Zheng, R.; Liu, H.; Zhang, X.; Guo, Z.; Xu, B. *J. Am. Chem. Soc.* **2004**, *126*, 9938−9939.

(11) (a) Dunford, H. B. *Heme Peroxidases*; Wiley−VCH: New York, 1999. (b) Welinder, K. G. *Curr. Opin. Struct. Biol.* **1992**, *2*, 388−393. (c) Gajhede, M.; Schuller, D. J.; Henriksen, A.; Smith, A. T.; Poulos T. L. *Nat. Struct. Biol.* **1997**, *4*, 1032−1038. (d) Kurosaka, A.; Yano, A.; Itoh, N.; Kuroda, Y.; Nakagawa, T.; Kawasaki, T. *J. Biol. Chem.* **1991**, *266*, 4168−4172. (e) van Huystee, R. B.; McManus, M. T. *Glycoconjugate J.* **1998**, *15*, 101−106. (f) Takahashi, N.; Lee, K. B.; Nakagawa, H.; Tsukamoto, Y.; Masuda, K.; Lee, Y. C. *Anal. Biochem.* **1998**, *255*, 183−187. (g) Veitch, N. C.; Smith, A. T. *Adv. Inorg. Chem.* **2001**, *51*, 107−162.

(12) (a) Gazaryan, I. G.; Klyachko, N. L.; Dulkis, Y. K.; Ouporov, I. V.; Levashov, A. V. *Biochem. J.* **1997**, *328*, 643−647. (b) Ferapontova, E. E.; Grigorenko, V. G.; Egorov, A. M.; Börchers, T.; Ruzgas, T.; Gorton, L. *J. Electroanal. Chem.* **2001**, *509*, 19−26.

carboxylic acid-terminated clusters were insoluble in toluene and were separated by centrifugation, and washed several times with toluene and once with 1-propanol to remove reaction byproducts. The purified clusters were redissolved in an aqueous solution of pH 10 containing 20 mM of HEPES (*N*-(2-hydroxyethyl)piperazine-*N*′-(2-ethanesulfonic acid), Sigma).

2.2. Modification with Nitrilotriacetic−Co(II). The amino-nitrilotriacetic−Co(II) complex (ANTA−Co^{2+}) was formed by reaction of N_α,N_α-bis(carboxymethyl)-L-lysine hydrate (ANTA, Fluka) with an excess of cobalt(II) chloride (Sigma) in 20 mM HEPES in aqueous solution. The cobalt excess was precipitated by increasing the pH to 10, and the hydroxide was removed by filtration through a 0.2 μm membrane (PTFE, Amicon). Activation of the carboxylate groups of the Au−TA clusters and subsequent amidation of the NHS-esters with the ANTA−Co(II) complex was performed overnight in a single step in the presence of 3 mM *N*-hydroxysuccinimide (NHS, Fluka) and 3 mM 1-ethyl-3-[3′-(dimethylamino)propyl]carbodiimide (EDC, Sigma) in 20 mM HEPES buffer (pH 7.5).[13] Further Au−TA−ANTA−Co(II) purification was carried out by ultrafiltration through low-adsorption hydrophilic 30 000 NMWL cutoff membranes (regenerated cellulose, Amicon).

2.3. Specific Immobilization of Histidine-Tagged Enzymes on Au−TA−ANTA−Co(II). A six-histidine tag was introduced at the N-terminus of the protein HRP by genetic engineering (N_{His}-HRP_{rec}), providing complementarity with the transition metal complex. Non-glycosylated recombinant HRP_{rec} and recombinant N_{His}-HRP_{rec} were produced in *E. coli* and refolded from inclusion bodies as described in ref 12. The enzymes displayed activities of 1240 and 1200 U mg^{-1}, respectively, toward ABTS (2,2′-azino-bis(3-ethylbenzothiazoline-6-sulfonic acid) diammonium salt). Wild-type enzyme (HRP_{nat}) was from a commercial source (HRP purified type VI, 1000 U mg^{-1} ABTS, Sigma).

FNR protein was modified with a histidine pair (His−X_3−His) in a surface-exposed α-helix of the NADPH binding domain by site-directed mutagenesis according to previous work.[9e] The FNR mutant (K290H/K294H, FNR-II) displayed an activity of 20 U mg^{-1} toward 2,6-dichlorophenol-indophenol (DCPIP; Sigma).[14]

Enzymatic binding was carried out by incubation of the functionalized nanoparticles in 0.1 mg cm^{-3} solutions of HRP_{rec}, N_{His}-HRP_{rec}, HRP_{nat}, or FNR-II in 50 mM phosphate buffer, 0.1 M KCl, pH 7.5 for 1 h at room temperature. Au−TA−ANTA−Co^{2+}−protein nanoparticles were separated from unbound enzyme molecules by ultrafiltration through low-adsorption hydrophilic 100 000 NMWL cutoff membranes (Amicon).

The activity of the nanoparticle−enzyme conjugates was determined spectrophotometrically. For HRP, the change in absorbance at 405 nm was monitored for its reaction with 8.6 mM ABTS as electron donor and 3 mM H_2O_2 as electron acceptor in 100 mM potassium phosphate buffer (pH 5.0) at 25 °C. In the case of FNR, the reaction with 0.035 mM 2,6-dichlorophenol-indophenol (DCPIP; Sigma) as electron acceptor and 0.12 mM NADPH (Sigma) as electron donor in 50 mM phosphate buffer (pH 7.5) at 25 °C was monitored at 600 nm.

2.4. FTIR Spectroscopy Measurements. Nanoparticle samples at the different chemical modification stages were concentrated by ultrafiltration and after resuspension in an aqueous solution at pH ≈ 9 were evaporated to dryness on a polished CaF_2 window. The IR spectra were recorded in a Nicolet 860 Fourier transform spectrometer equipped with an MCT detector and a purge gas system for removal of CO_2 and H_2O (Whatman). The IR spectra were averaged over 124 scans; the spectral resolution was 2 cm^{-1}. The spectra were blank subtracted and baseline corrected using OMNIC software from Nicolet.

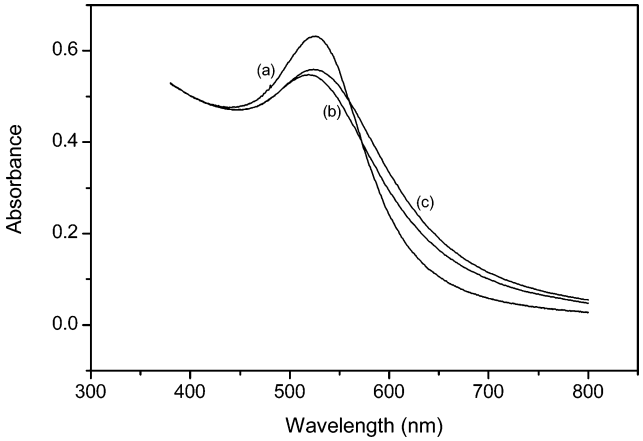

Figure 1. UV−vis absorption spectra for gold nanoparticles: (a) $(C_8H_{17})_4N^+Br^-$-stabilized in toluene; (b) transferred to water using thioctic acid in 20 mM HEPES buffer, pH 7.5; (c) assembly Au−TA−ANTA−Co(II) in 20 mM HEPES buffer, pH 7.5.

2.5. Transmission Electron Microscopy (TEM). The morphology and size distribution of the nanoparticles were studied in a Zeiss-EM902A transmission electron microscope using an acceleration voltage of 200 kV. The samples for examination by TEM were prepared by evaporation of a drop of nanoparticle solution on carbon films supported on standard copper grids. Mean particle size and standard deviation were determined from measurements of at least 100 particles.

2.6. pH-Induced Flocculation. The stability of nanoparticle solutions as a function of solution pH was studied by UV−visible spectroscopy using a Uvikon spectrophotometer. Identical nanoparticle solution aliquots were added to fixed volumes of buffer solution, after which the pH was adjusted.

3. Results and Discussion

3.1. Water-Dispersible Gold Nanoparticles. The underivatized gold nanoparticles prepared in toluene had a moderately narrow size distribution (particle diameter of (3.1 ± 1.3) nm as determined by TEM) and showed a characteristic surface plasmon band at 526 nm (Figure 1, curve a). FTIR characterization (see Supporting Information) confirmed the presence of the phase-transfer reagent ($(C_8H_{17})_4N^+Br^-$).[15]

The transfer of gold nanoparticles to water was initially carried out following a variation of the procedure described by Gittins et al.[5c] using 11-mercaptoundecanoic acid (MUA). Addition of an ω-mercaptocarboxylic acid precipitates the particles from the toluene dispersion due to their functionalization and the consequent polarity change of the ligand termination. The resulting Au−MUA clusters had an average core diameter of (3.4 ± 0.8) nm based on TEM analysis (see Supporting Information). Stable sols were obtained using this ligand and have been used for nonspecific attachment of biomolecules through noncovalent electrostatic interactions.[5c] Unfortunately, the further chemical modification of the particle ligand shell in the strategy shown in Scheme 1 requires a pH of 7.5,[13] where flocculation occurs, and therefore the Au−MUA clusters could not be employed for protein immobilization.

In view of their lower pK_a values,[16] the use of short-length thio acids was subsequently assessed for nanoparticle transfer. Experiments using 3-mercaptopropionic acid led to unstable

(13) (a) Cuatrecasas, P.; Parikh, I. *Biochemistry* **1972**, *11*, 2291−2298. (b) Tedder, J. M.; Nechvatal, A.; Murray, A. W. Amino acids and proteins. In *Basic organic chemistry*; John Wiley & Sons: London, 1972; Chapter 6, pp 305−342.
(14) Koike, M.; Hayakawa, T. *Methods Enzymol.* **1970**, *18*, 298−307.
(15) (a) Fink, J.; Kiely, C. J.; Bethell, D.; Schiffrin, D. J. *Chem. Mater.* **1998**, *10*, 922−926. (b) Nikoobakht, B.; El-Sayed, M. A. *Langmuir* **2001**, *17*, 6368−6374.
(16) *CRC Handbook of Chemistry and Physics*, 82nd ed.; CRC Press: Boca Raton, FL, 2001.

Figure 2. TEM image of TA-derivatized gold nanoparticles after transfer into water.

colloids, which may be ascribed to the known tendency of very short chain alkanethiolates to form disordered structures.[17] In contrast, greatly improved stability was obtained using thioctic acid (TA, 1,2-dithiolane-3-pentanoic acid). Cyclic disulfide SAMs are more stable than those obtained with single thiol or acyclic disulfide units, a consequence of the anchoring of the ligand to the metal core surface through two sulfur atoms.[18] Dithiolane sulfur atoms chemisorb strongly to Au, thereby displacing the phase-transfer reagent from the surface.[19] The observed shift to lower wavelengths in the plasmon band position (Figure 1, curve b) is a consequence of the change in both the dielectric permittivity of the ligand shell and the refractive index of the solvent.[20] The choice of buffer, however, had no significant effect on the value of λ_{max}.

FTIR measurements (see Supporting Information) demonstrate the complete exchange of TOABr by thioctic acid molecules on the clusters.[21] TEM characterization of Au−TA clusters (Figure 2) showed a fairly monodisperse particle size distribution with an average diameter of (2.9 ± 0.8) nm. Elemental analysis showed a composition of 81.9% gold and 1.7% sulfur corresponding to a surface coverage by sulfur atoms of $(6.2 \pm 0.5) \times 10^{-10}$ mol cm^{-2} close to a reported monolayer thiolate surface coverage of 7.6×10^{-10} mol cm^{-2} on Au(111).[22] The absence of N and Br provides additional support for the analysis of the FTIR results.

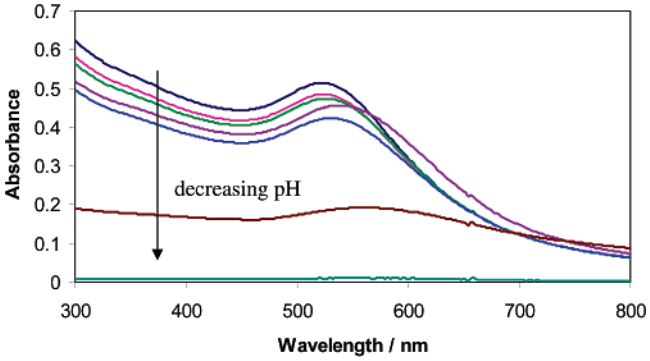

Figure 3. UV−vis absorption spectra for Au−TA clusters in aqueous solutions of different pH (between 5.8 and 7, with increments of 0.2 pH units).

Stability of the colloid at the pH values required for further functionalization is a crucial feature of the functionalization strategy. Therefore, flocculation studies were carried out as a function of pH. To ascertain the longer-term stability of the sols, measurements were carried out 24 h after pH adjustment. It is well documented[23] that protonation of the terminal carboxylate groups on the clusters causes flocculation and the emergence of a second plasmon absorption band due to optically coupled dipoles. The separation between the first (single-particle) and second (coupled-particle) plasmon bands depends on the length of the spacer, in this case the ligand, as was recently demonstrated using ω-mercaptoacids of different chain lengths.[24] A very small interparticle distance results in a clearly resolved second band, whereas longer spacers bring about merely a shoulder under the long-wavelength flank of the primary band.

The results in Figure 3 show that the particles remain in solution down to pH values of 6.2, because the absorbance remains fairly constant. With increasing acidity of the solution, a red shift and broadening of the peak occur, indicating flocculation. For pH 6.0 and below, however, the pH-induced aggregation becomes sufficiently important to precipitate the nanoparticles out of the solution. This pH value is in accordance with the increase in the pK_a of ω-mercaptoacids when present as a ligand as compared to its solution value [pK_a(TA, solution) $\approx$ 5, pK_a(TA, SAM) $\approx$ 6.5].[25] For the present work, however, the operational pH window where the functionalized clusters remained dissolved was more than adequate for further modification chemistry.

3.2. Stepwise Construction of Nanoparticles with Co(II)-Terminated Ligands. Au−TA particles proved an excellent building platform for a tailored SAM for specific protein immobilization. The terminal carboxylate groups in the capping ligands were activated by esterification with *N*-hydroxysuccinimide catalyzed by EDC in HEPES buffer, a well-established method[13] to facilitate the covalent linkage of the ANTA−Co(II) complex (Scheme 1) through the free amino groups. The FTIR spectra of the Au−TA−ANTA−Co(II) assembly shown

(17) Porter, M. D.; Bright, T. B.; Allara, D. L.; Chidsey, C. E. D. *J. Am. Chem. Soc.* **1987**, *109*, 3559−3568.
(18) (a) Letsinger, R. L.; Elghanian, R.; Viswanadham, G.; Mirkin, C. A. *Bioconjugate Chem.* **2000**, *11*, 289−291. (b) Yonezawa, T.; Yasui, K.; Kimizuka, N. *Langmuir* **2001**, *17*, 271−273.
(19) Porter, L. A., Jr.; Ji, D.; Westcott, S. L.; Graupe, M.; Czernuszewicz, R. S.; Halas, N. J.; Lee, R. *Langmuir* **1998**, *14*, 7378−7386.
(20) (a) Underwood, S.; Mulvaney, P. *Langmuir* **1994**, *10*, 3427−3430. (b) Templeton, A. C.; Pietron, J. J.; Murray, R. W.; Mulvaney, P. *J. Phys. Chem. B* **2000**, *104*, 564−570.
(21) Lin, S. Y.; Tsai, Y. T.; Chen, C. C.; Lin, C. M.; Chen, C. H. *J. Phys. Chem. B* **2004**, *108*, 2134−2139.
(22) Walczak, M. M.; Popenoe, D. D.; Deinhammer, R. S.; Lamp, B. D.; Chung, C.; Porter, M. C. *Langmuir* **1991**, *7*, 2687−2693.
(23) (a) Weisbecker, C. S.; Merritt, M. V.; Whitesides, G. M. *Langmuir* **1996**, *12*, 3763−3772. (b) Mayya, K. S.; Patil, V.; Sastry, M. *Langmuir* **1997**, *13*, 3944−3947.
(24) (a) Bellino, M. G.; Calvo, E. J.; Gordillo, G. *Phys. Chem. Chem. Phys.* **2004**, *6*, 424−428. (b) Zhong, Z.; Patskovskyy, S.; Bouvrette, P.; Luong, J. H. T.; Gedanken, A. *J. Phys. Chem. B* **2004**, *108*, 4046−4052.
(25) Wang, Y.; Kaifer, A. E. *J. Phys. Chem. B* **1998**, *102*, 9922−9927.

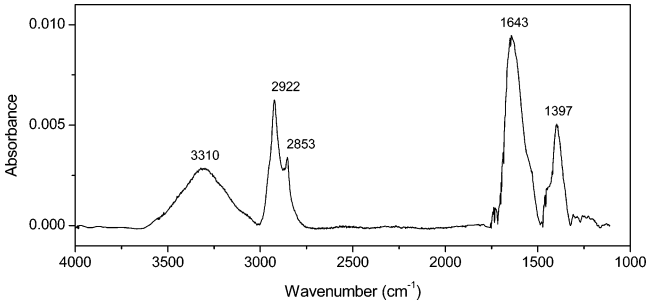

Figure 4. FTIR spectrum of the complete nanointerface Au−TA−ANTA−Co(II). Peaks at 3310, 2922, 2853, 1643, and 1397 cm^{-1} correspond to vibrational modes of $\nu(-NH)$, $\nu_{asy}(-CH_2)$, $\nu_{sym}(-CH_2)$, $\nu_{amide\ I\ band}(-CO)$, and $\nu_{sym}(-CO_2^-)$, respectively. Nanoparticles were drop-cast on a CaF_2 window.

in Figure 4 display characteristic amide bands together with vibrational modes associated with the NTA carboxylate groups. It confirms the functionalization of nanoparticles with nitrilotriacetic groups complexed with cobalt(II) ions. This chelation, causing partial neutralization of the carboxylic acid groups, may be responsible for the slight blue shift of the UV−vis spectrum (Figure 1, curve c). The tailored Au clusters obtained formed stable solutions in physiological buffers commonly employed for protein immobilization at pH > 6, such as PBS (phosphate buffer saline) or HEPES.

3.3. Enzyme Immobilization on the Au−TA−ANTA−Co(II) Assembly. Functionalized nanoparticles were tested for specific protein immobilization of deglycosylated N_{His}-HRP_{rec}, which bears a metal binding site (six-histidine tag) obtained by genetic engineering. The ANTA−Co(II) complex termination contains two free coordination sites occupied by water molecules that can be replaced by histidine residues (Scheme 1).[26]

Evidence of protein binding to the functionalized nanoparticles was obtained by analysis of its enzymatic activity. The method relies on a catalytic cycle in which the peroxidase enzyme is first oxidized by H_2O_2, and subsequently reduced by ABTS. The oxidation product of ABTS shows a strong absorbance at 405 nm, which was monitored spectrophotometrically. Co(II)-terminated nanoparticles that were incubated in the presence of N_{His}-HRP_{rec} produced an increase in the absorption at this wavelength (Figure 5, curve a) when reacted with H_2O_2 and ABTS, thus providing clear evidence that the enzyme is immobilized.

The degree of enzyme functionality after immobilization as well as the degree of protein immobilization was assessed in a separate experiment (Figure 6, Table 1). The enzymatic activity of the protein before immobilization is almost entirely retained after attachment to the Co(II)-terminated nanoparticles, showing that the immobilization strategy preserves fully the biological function. In addition, the supernatant loses virtually all enzymatic activity after immobilization, further demonstrating that protein attachment is quantitative.

Two independent control experiments were carried out to demonstrate that the immobilization results specifically from interaction between the cobalt complex and the six-histidine tag and that nonspecific protein adsorption through electrostatic, hydrophobic, or hydrogen-bonding interactions does not occur.[27] The attachment of the enzyme through Co(II)-His coordination was confirmed by incubation of Co(II)-terminated nanoparticles in a solution of nonglycosylated HRP_{rec} without the histidine

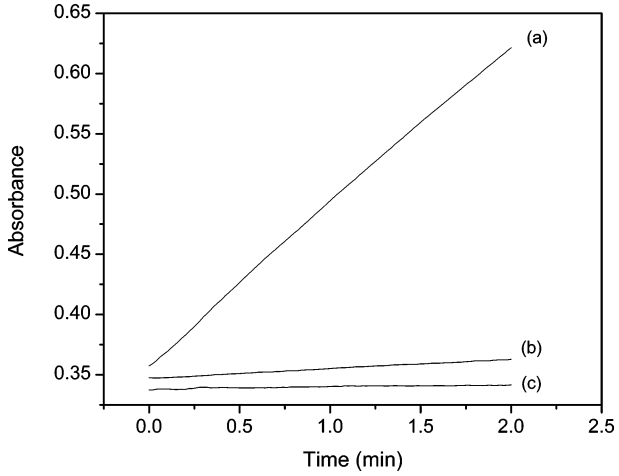

Figure 5. Activity of HRP enzyme molecules immobilized by the constructed nanointerface Au−TA−ANTA−Co(II) after incubation in: (a) N_{His}-HRP_{rec} (histidine-tagged HRP); (b) HRP_{rec}; (c) HRP_{nat}. Conditions: 8.6 mM ABTS as electron donor and 3 mM H_2O_2 as electron acceptor in 100 mM potassium phosphate buffer, pH 5.0 at 25 °C. Wavelength 405 nm.

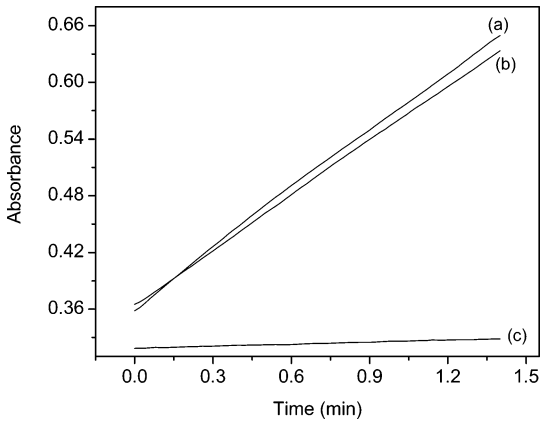

Figure 6. Activity of HRP enzyme: (a) before immobilization; (b) after immobilization by the functionalized nanoparticles Au−TA−ANTA−Co(II); (c) activity in the supernatant solution. Conditions: 8.6 mM ABTS as electron donor and 3 mM H_2O_2 as electron acceptor in 100 mM potassium phosphate buffer, pH 5.0 at 25 °C. Wavelength 405 nm.

Table 1. Enzymatic Activities (Absolute and as a Percent of the Initial Activity) before and after Protein Immobilization onto Au−TA−ANTA−Co(II) Nanoparticles

	N_{His}-HRP_{rec}		FNR-II	
	U mL^{-1}	%	U mL^{-1}	%
initial	0.28	100	13.1	100
immobilized	0.26	93	12.7	97
supernatant	0.01	4	0.1	1

tag. Figure 5, curve b, shows the absence of absorbance changes and therefore demonstrates that the six-histidine tag is essential for protein immobilization. Because deglycosylated proteins are prone to adsorption through electrostatic and/or hydrophobic interactions,[27] this experiment also provides evidence that these types of nonspecific binding interactions do not occur.

The absence of nonspecific adsorption through hydrogen bonding was checked using glycosylated HRP_{nat} without the

(26) Porath, J.; Carlsson, J.; Olsson, I.; Belfrage, G. *Nature* **1975**, *258*, 598−599.
(27) (a) Yoon, J.-Y.; Kim, J.-H.; Kim, W.-S. *Colloids Surf., B* **1998**, *12*, 15−22. (b) Nakanishi, K.; Sakiyama, T.; Imamura, K. *J. Biosci. Bioeng.* **2001**, *91*, 233−244.

histidine tag. The sugar groups on the glycosylated enzyme make the molecule hydrophilic and particularly suited for this control experiment. Again, negligible changes in absorbance were observed (Figure 5, curve c), which demonstrates that the present immobilization strategy is altogether insensitive to nonspecific protein adsorption. The observed nonspecific binding results contrast greatly with the known adsorption of all of the forms of HRP tested here (i.e., native, deglycosilated, N-His-tagged), which are known to bind strongly to bare gold surfaces.[28]

To extend the methodology presented here to other proteins, the immobilization of ferredoxin-$NADP^+$ reductase protein (FNR) genetically modified with a histidine pair was tested. Functionalized Co(II)-terminated nanoparticles were incubated with the FNR-II mutant protein. Evidence of the binding of the mutant protein onto the gold nanoparticle was obtained by analysis of diaphorase activity with NADPH as electron donor and DCPIP as electron acceptor. Table 1 shows that FNR-II was also immobilized to a high extent onto the gold nanoparticles and fully functional. Nonspecific protein adsorption was not observed with native FNR without a histidine pair (data not shown). These results further support the practical value and applicability of the approach presented.

The importance of this work is to have demonstrated a stepwise nanoparticle derivatization strategy that provides a method for a specific and oriented protein immobilization that preserves biological functionality and avoids nonspecific adsorption, thus allowing the construction of complex biofunctional nanoassemblies.

4. Conclusion

Synthesis of gold nanoparticles in toluene and their transfer to water by thioctic acid modification have been proven to be an efficient method for obtaining stable low-dispersity nanoparticles that are a good platform for easy stepwise building of versatile functional nanointerfaces. The specific immobilization of His-tagged proteins was demonstrated for the cases of genetically engineered horseradish peroxidase and ferredoxin-$NADP^+$ reductase, confirming fully functional attachment of the protein to the NTA-Co(II)-platform. This methodology is readily applicable to other proteins. These functionalized nanoparticles thus represent an attractive ready-to-use tool for protein immobilization on nanoparticles.

Acknowledgment. We are grateful to Dr. I. Gazaryan for supplying recombinant peroxidases, to Dr. C. Gómez-Moreno for FNR proteins, and to Dr. A. L. de Lacey for critical reading of the manuscript. J.M.A. acknowledges support from a Consejería de Educación de la Comunidad Autónoma de Madrid postdoctoral fellowship, co-financed by the European Social Fund, and a postdoctoral fellowship from Fundación Ramón Areces. M.P. acknowledges receipt of a Ph.D. fellowship from the Consejería de Educación de la Comunidad Autónoma de Madrid, co-financed by the European Social Fund. S.F.L.M. and D.J.S. acknowledge financial support from the EU Research Training Network SUSANA (Supramolecular Self-Assembled Interfacial Nanostructures) under contract HPRN-CT-2002-00185. V.M.F. acknowledges financial support from an intramural CSIC project under contract CSIC-200450F0340.

Supporting Information Available: FTIR spectra of $(C_8H_{17})_4N^+Br^-$-stabilized and TA-capped gold nanoparticles; TEM analysis of 11-mercaptoundecanoic acid-capped gold nanoparticles (Au−MUA clusters). This material is available free of charge via the Internet at http://pubs.acs.org.

JA042717I

(28) (a) Ferapontova, E.; Gorton, L. *Electroanalysis* **2003**, *15*, 484−491. (b) Ferapontova, E.; Gorton, L. *Bioelectrochemistry* **2002**, *55*, 83−87. (c) Ferapontova, E. E.; Grigorenko, V. G.; Egorov, A. M.; Börchers, T.; Ruzgas, T.; Gorton, L. *Biosens. Bioelectron.* **2001**, *16*, 147−157.